hypoxic condition and VHL cannot recognize HIF-1α as a target, resulting in a reduced rate of degradation.[17,18] The stabilized HIF-1α interacts with the constitutively expressed HIF-1β protein and induces the expression of certain genes such as VEGF[3], glycolytic enzyme[4] and erythropoietin.[19] The induction of these genes is triggered by the interaction of HIF-1 with its cognate DNA recognition site, that is, the hypoxia-response element (HRE).[3,20] Previously, Shibata *et al.* developed an artificial hypoxia-inducible promoter system using five copies of HRE (5HRE) derived from the VEGF promoter and the human cytomegalovirus minimal promoter (CMVmp), and demonstrated that the 5HRE promoter increased gene expression by a factor of more than 500 under hypoxic conditions *in vitro*.[21,22]

In the process of developing radiosensitizers, 2-nitroimidazole derivatives have been found to accumulate in hypoxic cells of solid tumors. Consequently, some methods to obtain quantitative or qualitative data about tumor hypoxia have been developed, and suitably labeled 2-nitroimidazole analogues have been utilized to develop a variety of non-invasive monitoring systems for tumor hypoxia, *e.g.* magnetic resonance spectroscopy (MRS)[23,24], positron emission tomography (PET)[25] and single photon electron capture tomography (SPECT).[25] Pimonidazole, a well-known hypoxia marker, is also a 2-nitroimidazole derivative and has been developed for the immunohistochemical analysis of tumor specimens.[26,27] Polarographic microelectrodes can directly record the oxygen status of tumor tissues and have therefore been widely used in clinical practice for cancer patients.[27] Although all of these methods yield detailed information about tumor hypoxia, they do not accurately reflect HIF-1 activity because HIF-1 activation is caused by not only intratumoral hypoxia but also by genetic alterations, such as gain-of-function mutations in oncogenes and loss-of-function mutations in tumor-suppressor genes.[28] Moveover, growth factors and cytokines stimulate HIF-1α synthesis via the oxygen-independent activation of phosphatidylinositol 3-kinase (PI3K)[29,30] or mitogen-activated protein kinase (MAPK) pathways.[31] VHL mutation also leads to over expression of the HIF-1α protein.[32] Therefore, lack of a routine, easy and dynamic method to monitor HIF-1 activity in solid tumors remains a major problem.

In the present study, we developed a suitable and convenient system to monitor HIF-1 activity in real-time in tumor xenografts by using the 5HRE promoter.[21,22] Destabilized Enhanced GFP (d2EGFP) was chosen as the reporter gene because it can be detected without any substrate or cofactor, and especially because the half-life of d2EGFP is reduced to less than 2 hours. Such short half-life is due to the residues 422–461 of mouse ornithine decarboxylase protein (MODC domain) fused in d2EGFP protein, and makes it possible to observe HIF-1 activity in real-time.[33] We were consequently able to demonstrate that d2EGFP fluorescence is observed *in vitro* only under hypoxic conditions and *in vivo* in the regions stained with the hypoxia marker.

MATERIALS AND METHODS

DNA constructs

The DNA fragments encoding EGFP and d2EGFP were inserted between the NcoI and NotI recognition sites of the pEF/myc/cyto vector (Invitrogen, Carlsbad, CA) to construct the plasmids pEF/EGFP and pEF/d2EGFP, respectively. In addition, the DNA fragment of the 5HRE-hCMVmp enhancer/promoter[22] was inserted between the KpnI and NcoI sites of pEF/EGFP and pEF/d2EGFP to construct the plasmids p5HRE-EGFP and p5HRE-d2EGFP, respectively. To construct the plasmid, pCMV-d2EGFP, the DNA fragment of the 5HRE-hCMVmp enhancer/promoter of p5HRE-d2EGFP was substituted for that of the intact CMV promoter.[22]

Cell culture and transfection

The human melanoma cell line Be11[34] (the gift from Dr. Oya) was cultured in 20% FCS-MEM-1. To establish the stable transfectants, the cells were seeded on a 60mm culture dish and transfected with 5 μg of pCMV-d2EGFP, p5HRE-EGFP or p5HRE-d2EGFP by using the Superfect Transfection Reagent (QIAGEN, Valencia, CA), according to the manufacture's instructions. Three hours after the transfection, the culture medium was changed to the medium containing 800 μg/ml of G418 disulfate (Nacalai Tesque, Kyoto, Japan), an antibiotic to select the stable transfectant, and the cells were cultured for an additional 2 weeks. With the aid of a fluorescent microscope with a 488 / 510 filter, a stable transfectant with strong fluorescence was isolated from the cells transfected with pCMV-d2EGFP plasmid. The stable transfectant with p5HRE-d2EGFP, on the other hand, was treated under hypoxic conditions (0.02%) for 20 hours before being isolated.

Hypoxia treatment and reoxygenation

Cells were treated under various hypoxic conditions. In one procedure, 90% N_2, 5% H_2 and 5% CO_2 with a palladium catalyst were used in an Environment Chamber (Sheldon Manufacturing, Inc., Cornelius, OR). In another, the cells were treated in pre-warmed aluminum chambers by means of exhausting and gassing with 95% N_2 and 5% CO_2 for various cycles to produce oxygen concentrations of 2%, 0.2%, 0.02% and <0.01%. After the hypoxic treatment (0.02% O_2) for 20 hours, the cells were cultured in the incubator with 95% air and 5% CO_2 for the times indicated in each figures to reoxygenate the cells.

Flow cytometry analysis

Green fluorescence was analyzed with a flow cytometer (Becton Dickinson, San Jose, CA), and the data were processed with CellQuest software (Becton Dickinson). Histograms of GFP were plotted with the log scale for GFP fluo-

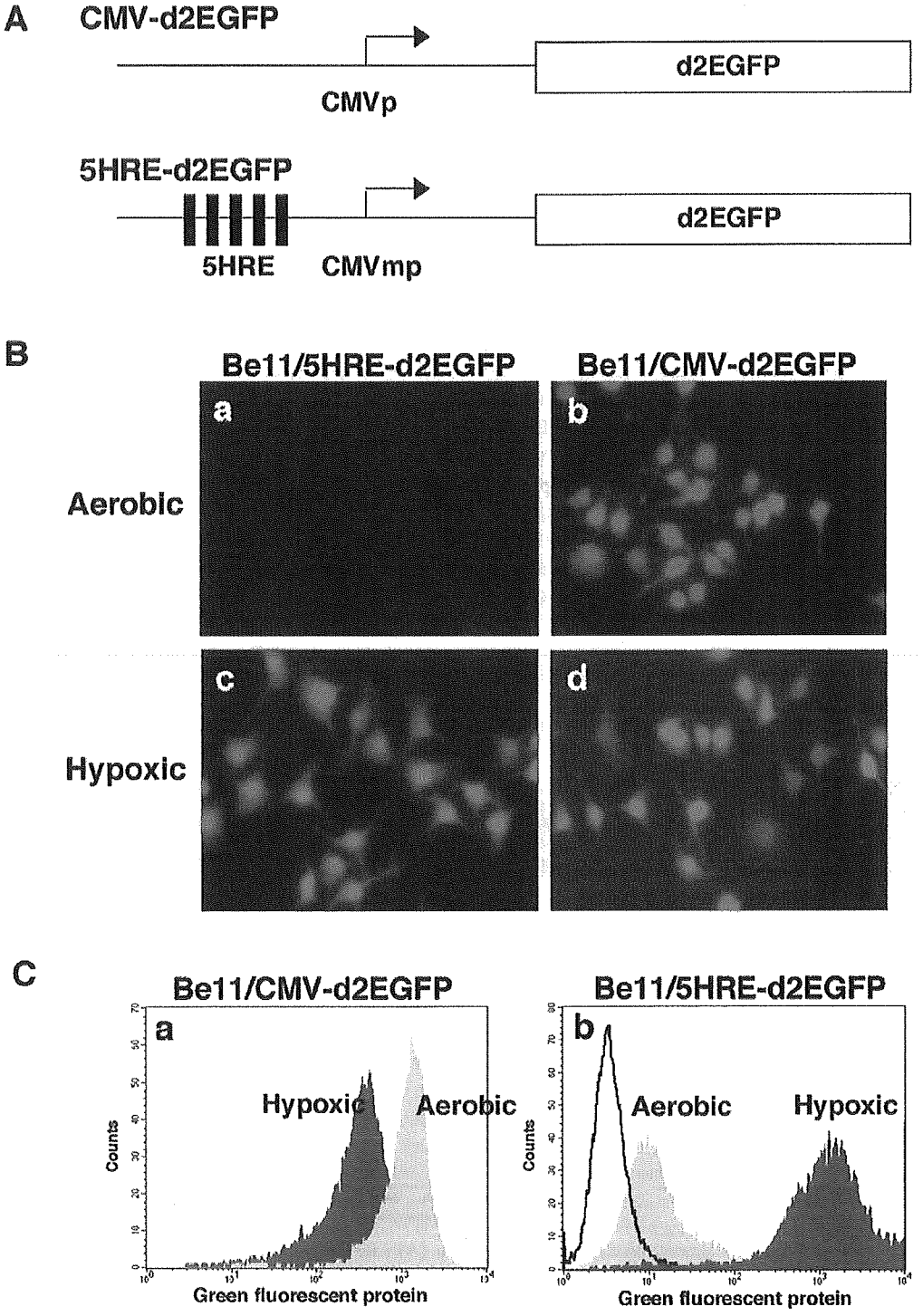

Fig. 1. Hypoxia-responsible d2EGFP expression in Be11/5HRE-d2EGFP stable transfectant. **(A)** Schematic diagrams of the CMV-d2EGFP gene (top) and the 5HRE-d2EGFP gene (bottom). **(B)** Both stable transfectants Be11/5HRE-d2EGFP (a, c) and Be11/CMV-d2EGFP (b, d) were treated under hypoxic condition (0.02% O_2) for 20 hours, and reoxygenated for 4 hours. **(C)** After the same treatment as described in (B), Be11/CMV-d2EGFP (a) and Be11/5HRE-d2EGFP (b) were subjected to FACS analysis and histograms of their fluorescent intensity are shown.

rescence and the results were recorded as means of the middle of the peaks.

Immunohistochemical analysis

Stable transfectants of Be11 with pCMV-d2EGFP or p5HRE-d2EGFP (10^6 cells in 100 µl of PBS) were subcutaneously (s.c.) injected into the flank or leg of 6–8 weeks nude mice (BALB/c nu/nu; CLEA Japan, Inc., Tokyo, Japan). When the tumor diameter exceeded 15 mm, the tumor bearing mice were intraperitoneally (i.p.) injected with pimonidazole hydrochloride[26,27] (60mg/kg), and 90 min later, the solid tumors were surgically removed and fixed in 10% Formalin Neutral Buffer Solution pH 7.4 (Wako Pure Chemical Industries, Osaka, Japan). Immunostaining for the detection of d2EGFP expression and hypoxic cells was carried out with the anti-GFP Ab (BD Living Color™ A.v. Peptide Antibody; Clontech, Franklin Lakes, NJ) and with anti-pimonidazole Ab (Hypoxyprobe-1 kit; Natural Pharmacia International, Inc., Belmont, MA), respectively, by the indirect immunoperoxidase method as described previously.[35] To calculate the percentage of pimonidazole-positive cells and d2EGFP-expressing cells in the Be11/5HRE-d2EGFP solid tumor, the corresponding pimonidazole-stained cells and d2EGFP-stained cells were quantified with NIH Image 1.63 software, and compared to the quantity of the whole tumor.

Fluorescent microscope analysis and imaging of HIF-1 activity in vivo

Microscopic analysis was conducted with an Olympus BX-60 microscope fitted with Olympus U-MWIB filter cubes (460–490 nm for excitation filter, 505–550 nm for dichroic filter and 515–550 for emission filter). Images were taken with a Sensys CCD Camera (Photometric, Livingston, UK). Blue color excitation light and yellow filters were used for the *in vivo* real-time imaging.

RESULTS

Hypoxia-inducible fluorescence from cells transfected with p5HRE-d2EGFP

To establish a convenient system to visualize the HIF-1 transcriptional activity in tumor xenografts in real-time, we first constructed the p5HRE-d2EGFP plasmid (Fig. 1A). A

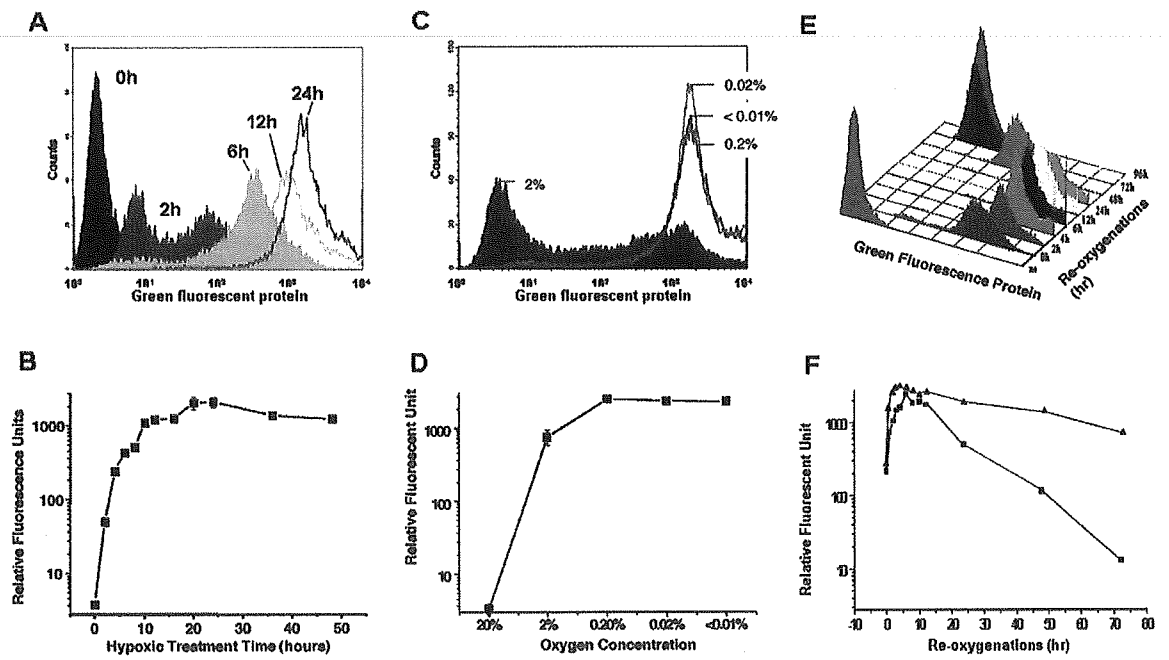

Fig. 2. Effects of various hypoxic treatments on d2EGFP fluorescence. **(A)** After hypoxic treatment (0.02% O_2) of various durations, fluorescent intensity of Be11/5HRE-d2EGFP stable transfectants was analyzed with FACS and is shown as a histogram. **(B)** Ratios of fluorescent intensity of the same cell preparations as in (A) to the intensity without hypoxic treatment are shown as relative fluorescence units. **(C)** After various hypoxic treatments (2%, 0.2%, 0.02% and <0.01%) for 20 hours, fluorescent intensity of Be11/5HRE-d2EGFP stable transfectants was analyzed and is shown as a histogram. **(D)** Ratios of fluorescent intensity of the cells after the same hypoxic treatments as in (C) to the intensity after aerobic treatment are shown as relative fluorescence units. **(E)** After hypoxic treatment (0.02% O_2) for 20 hours, Be11/5HRE-d2EGFP stable transfectants were reoxygenated for various durations and the fluorescent intensity was analyzed and is shown here as a histogram. **(F)** Ratios of fluorescent intensity of the cells after the same treatment as in (E) to the intensity after aerobic treatment are shown as relative fluorescence units. Be11/5HRE-EGFP stable transfectants (solid triangles), Be11/5HRE-d2EGFP stable transfectants (solid squares).

5HRE promoter was employed to induce reporter gene expression under the control of HIF-1 activity,[21,22] and d2EGFP was used as a reporter gene, because its half-life is reported to be somewhat less than 2 hours,[33] which we thought should enable us to observe HIF-1 activity in real-time. The human melanoma cell line Be11 was stably transfected with the plasmid p5HRE-d2EGFP, and a clone was isolated by taking advantage of the hypoxia-dependency of the d2EGFP expression (Fig. 1A). In addition, Be11, this time stably transfected with pCMV-d2EGFP plasmid, was established as a control with constitutive expression of d2EGFP (Fig. 1A). To confirm the occurrence of hypoxic induction, both stable transfectants were processed in 0.02% of oxygen concentration. The fluorescence microscopic examination clearly showed that Be11/5HRE-d2EGFP transfectants expressed negligible levels of fluorescence under aerobic conditions but adequate levels of fluorescence after hypoxic treatment (Fig. 1Ba and c). On the other hand, Be11/CMV-d2EGFP transfectants showed bright green fluorescence under both aerobic and hypoxic conditions (Fig. 1Bb and d).

FACS analysis also clearly showed fluorescent intensity in both cell lines (Fig. 1C). In the cell population of Be11/5HRE-d2EGFP transfectants, a more than 200-fold induction of d2EGFP fluorescence was observed after hypoxic treatment compared to after aerobic treatment (Fig. 1Cb), whereas constitutive fluorescence was observed after both aerobic and hypoxic treatment in the Be11/CMV-d2EGFP transfectants (Fig. 1Ca). These results indicate that the 5HRE-CMVmp promoter can be used as a specific and robust hypoxia-inducible promoter. Although hypoxic treatment itself seemed to somewhat diminish the brightness of the Be11/CMV-d2EGFP transfectants (Fig. 1Ca), such difference was hardly detectable by fluorescence microscopic analysis (Fig. 1Bb and d).

Effects of various hypoxic treatments on d2EGFP fluorescence

In order to analyze the effects of hypoxic treatment of various durations on fluorescent intensity, Be11/5HRE-d2EGFP transfectants were treated under hypoxic conditions for 0, 2, 6, 12, and 24 hours, after which the green fluorescence was monitored by means of FACS analysis. Even after 2 hours of hypoxic treatment, fluorescence was detected with fluorescent microscopic as well as with FACS analysis (Fig. 2A and data not shown). Increases in both fluorescent intensity and number of fluorescent cells depended on the duration of hypoxic treatment up to 24 hours, after which saturation levels were reached (Fig. 2A and B).

To assess the oxygen concentration required for inducing d2EGFP expression, Be11/5HRE-d2EGFP cells were treated for 20 hours with various oxygen concentrations, that is, <0.01%, 0.02%, 0.2% and 2%. FACS analysis showed that d2EGFP expression increased when the oxygen concentra-

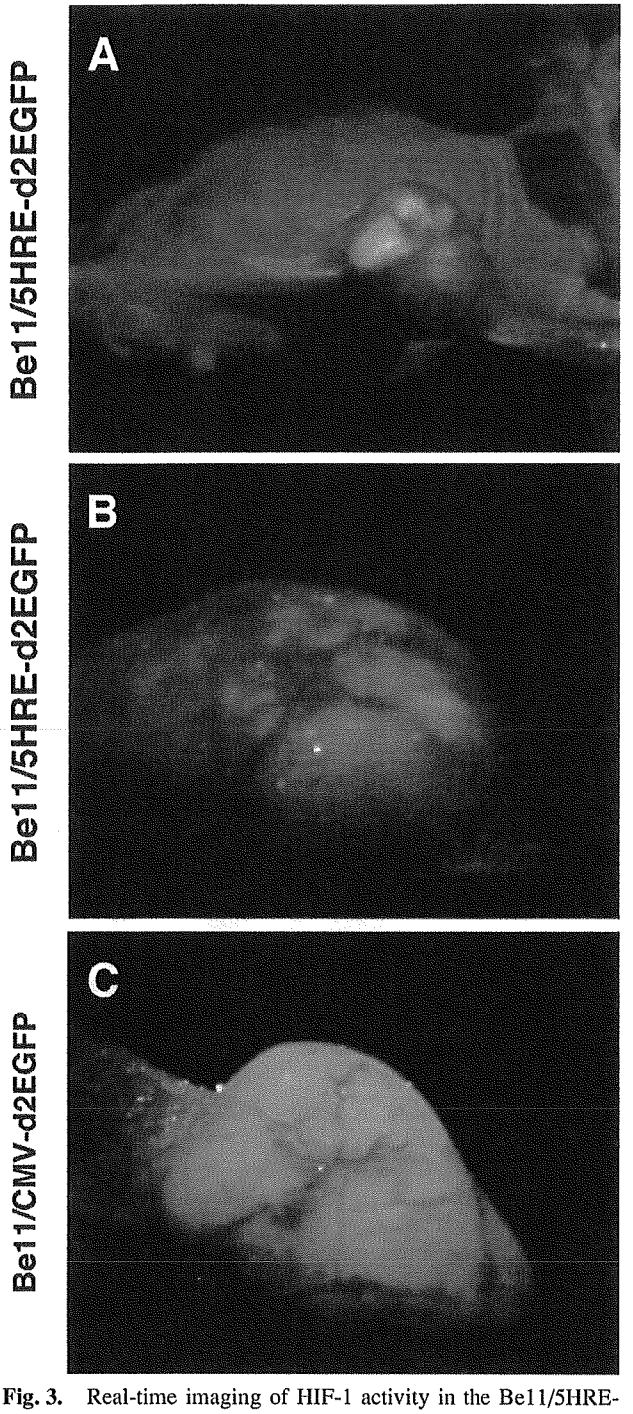

Fig. 3. Real-time imaging of HIF-1 activity in the Be11/5HRE-d2EGFP tumor xenograft. **(A), (B)** Heterogeneous fluorescence in the tumor xenograft with Be11/5HRE-d2EGFP cells was detected by means of blue excitation light and a yellow filter. **(C)** Homogeneous fluorescence in the tumor xenograft with Be11/CMV-d2EGFP cells was used as control.

tion was reduced from 20% to 0.2%, and maintained a high expression level from 0.2% to anaerobia (<0.01%) (Fig. 2C and D). Even at the 2% oxygen concentration, fluorescent intensity increased almost 1,000 times compared to the one at 20% oxygen concentration (Fig. 2D), and could be detected directly with the fluorescence microscope (data not shown).

Next we analyzed the effect of reoxygenation on d2EGFP fluorescence, because oxygen molecules are reported to be necessary for chromophore formation of GFP and its derivatives.[36] Be11/5HRE-d2EGFP cells were treated under hypoxic conditions (0.02% O_2) for 20 hours, and reoxygenated for various lengths of time in the incubator with 95% air and 5% CO_2. The hypoxic treatment even without any reoxygenation enhanced fluorescence by a factor of more than 200 compared to that observed under aerobic conditions (Fig. 2E and F). Reoxygenation for 4 hours resulted in a sharp and high peak of fluorescence, after which the fluorescence levels decreased dramatically. To examine the effect of the MODC domain fused in d2EGFP on protein stability, we established the Be11/5HRE-EGFP cells, in which expression of the EGFP protein (without MODC domain) was controlled by the 5HRE promoter. When the Be11/5HRE-EGFP cells were subjected to the same experiment as described above, they showed more stable fluorescence than the Be11/5HRE-d2EGFP cells during the observation period (Fig. 2F). These results clearly demonstrate that the decrease in the fluorescence of Be11/5HRE-d2EGFP was due to the MODC domain of the d2EGFP protein.

Real-time imaging of HIF-1 transcriptional activity in tumor xenograft

In order to visualize the HIF-1 transcriptional activity in a solid tumor in a living mouse, Be11/5HRE-d2EGFP cells were s.c. inoculated into nude mice. One month after the implantation, these cells formed solid tumors with diameter of more than 15 mm. Real-time imaging under the blue exci-

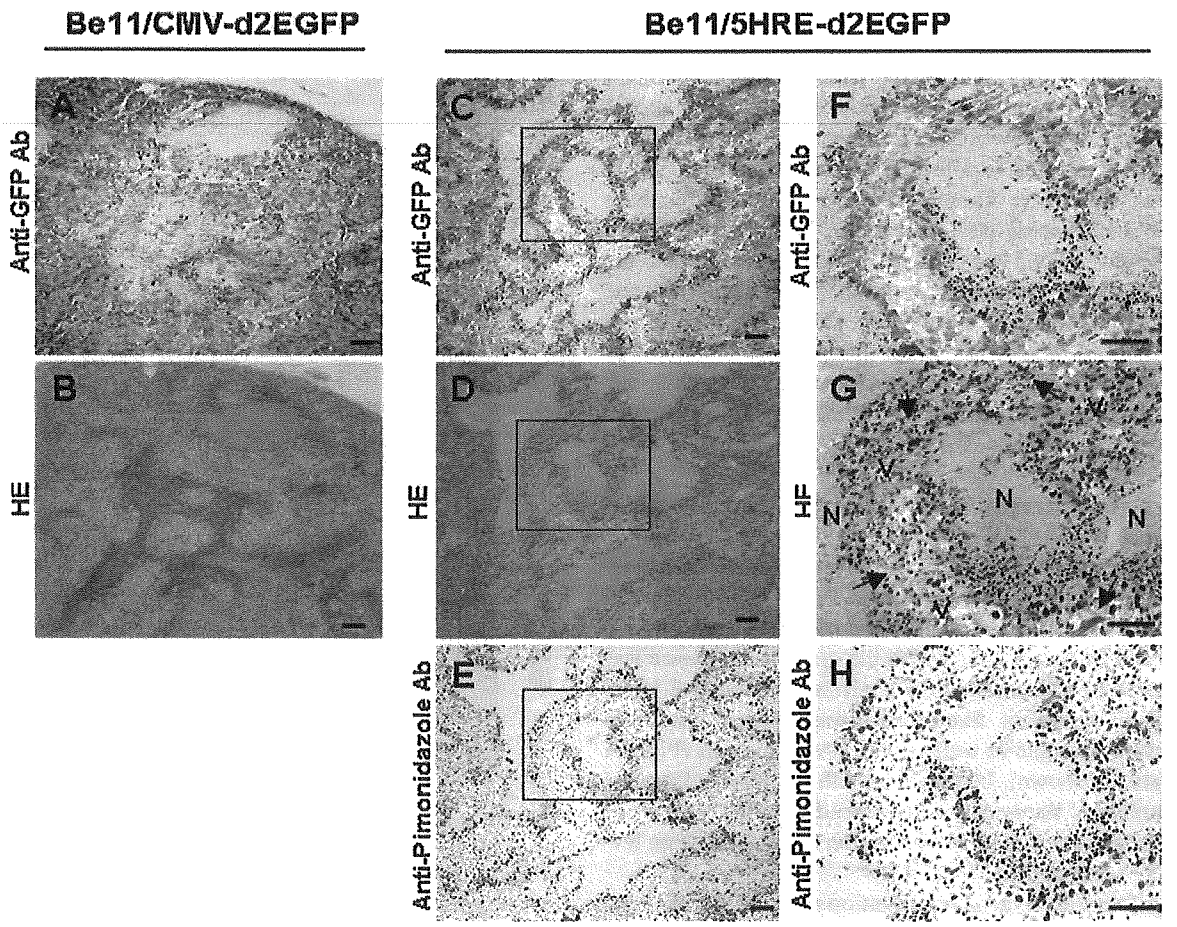

Fig. 4. Immunohistochemical analysis of d2EGFP-expressing cells in the Be11/5HRE-d2EGFP tumor xenograft. Tumor xenografts of Be11/CMV-d2EGFP cells (**A** and **B**) and Be11/5HRE-d2EGFP cells (**C-H**) were stained with anti-GFP Ab (**A, C** and **F**), HE (**B, D** and **G**) and anti-pimonidazole Ab (**E** and **H**). F, G and H show higher magnifications of the square areas in C, D and E, respectively. Bar = 100 μm. N = necrotic tumor tissue; V = well-oxygenated viable tumor tissue; arrow = blood vessel.

tation light showed heterogeneous, partition-dependent and weak green fluorescence in the tumor xenograft with Be11/5HRE-d2EGFP cells (Fig. 3A and B). In comparison, tumor xenografts with Be11/CMV-d2EGFP cells showed strong and homogeneous green fluorescence (Fig. 3C). No fluorescence was observed in the parental Be11 tumor (data not shown).

Characterization of GFP-expressing cells by immunohistochemical analysis

HIF-1 activation is induced by not only intratumoral hypoxia but also the other stimuli.[28–32] To determine, therefore, whether hypoxic stimuli definitely up-regulated the 5HRE-promoter activity in our *in vivo* study, the regions expressing d2EGFP in the solid tumor were compared to those stained with the hypoxic marker pimonidazole.[26,27] In the Be11/CMV-d2EGFP solid tumor, homogeneous and strong expressions of d2EGFP proteins were detected with the anti-GFP Ab, which recognizes all of GFP derivatives including d2EGFP (Fig. 4A). HE-stained section of Be11/CMV-d2EGFP xenograft revealed that the d2EGFP-expressing cells were in the viable regions (Fig. 4B). On the other hand, heterogeneous expressions of d2EGFP were observed in the tumor xenografts with Be11/5HRE-d2EGFP cells (Fig. 4C). The d2EGFP-positive cells were located in the boundary area between the well-oxygenated viable regions and the necrotic regions (Fig. 4C and D). Similar regions in the Be11/5HRE-d2EGFP tumor also stained with anti-pimonidazole Ab, (Fig. 4E).

Higher magnifications of the square areas in Fig. 4C, 4D and 4E are shown as Fig. 4F, 4G and 4H, respectively. In the HE-stained specimen, red blood cells clearly showed the location of tumor blood vessels (Fig. 4G), which were surrounded by viable tumor cells in direct proximity, and moreover by necrotic tumor cells at a greater distance. To be precise, the necrotic regions were located more than 100 μm from the blood vessels. In addition to the HE-stained specimens, the higher-magnified images stained with anti-GFP Ab clearly demonstrated that the d2EGFP-expressing cells were located about 100 μm from the tumor blood vessels (Fig. 4F). Finally, the staining pattern obtained with anti-GFP Ab was very similar to that produced by the hypoxia marker pimonidazole (Fig 4F and H). These results strongly suggest that the 5HRE-system induces d2EGFP expressions in hypoxic tumor cells.

In the specimens stained with anti-GFP Ab and anti-pimonidazole Ab, it was also clear that more cells were stained with the former than with the latter. For quantification, both specimens were analyzed with NIH Image 1.63 software. The percentage of pimonidazole-positive cells in the whole solid tumor was $9.2 \pm 3.8\%$ ($n = 5$), while that of d2EGFP-expressing cells in the whole solid tumor was significantly higher, $22.7 \pm 6.1\%$ ($n = 5$; $p < 0.01$).

DISCUSSION

HIF-1 induces various kinds of hypoxia-responsive gene expressions, which are related to the malignant phenotype of tumor cells, such as angiogenesis, metastasis, invasion and evasion of apoptosis.[3–5] The lack of a technique that allows for convenient imaging of HIF-1 transcriptional activity therefore remains as one of the problems for basic research aiming at the development of anticancer drugs in cancer treatment. In order to address this issue, we developed an imaging system using both an HIF-1-responsive promoter and a specific reporter protein. Shibata *et al.* examined various combinations of HRE and promoters to achieve higher responsiveness of promoter activity to hypoxic stress, and demonstrated that the combination of 5HRE and a CMVmp induces 500 fold more gene expression under hypoxic conditions than under aerobic conditions. Moreover, the expression level under hypoxic conditions is almost same as the one by the intact CMV promoter.[22] We therefore employed the 5HRE-hCMVmp enhancer/promoter system for the study presented here. In agreement with previously reported results,[22] only negligible levels of reporter expression were observed under aerobic conditions but these levels became clearly detectable after hypoxic treatment. For this reason, the 5HRE enhancer/promoter met our requirements better than any other regulatory systems.

We chose a derivative of GFP protein as the reporter gene because no additional cofactor or substrate is needed for its visualization. Attention must be paid, however, to applying GFP derivatives to *in vivo* imaging because anoxic conditions inhibit chromophore formation.[36] In fact, we observed in the FACS analyses that hypoxic treatment itself seemed to diminish the brightness of the Be11/CMV-d2EGFP transfectants somewhat (Fig. 1Ca), and that d2EGFP fluorescence increased after reoxygenation (Fig. 2E and F). But when we treated the cells with the translation inhibitor, cyclohexamide, just after the hypoxic treatment, the d2EGFP signal did not increase after reoxygenation (data not shown). This finding suggests that the increase in fluorescence after reoxygenation was not mainly the result of chromophore formation but of translation. We can therefore conclude that chromophore formation was not significantly inhibited in our experimental setting. Additionally, such small differences in fluorescent intensity were hardly detectable with fluorescence microscopic analysis (Fig. 1Bb and d). Thus, there seemed to be no serious obstacles to employing d2EGFP as a reporter for our purpose.

The 5HRE enhancer/promoter system has been used to analyze the effect of x-ray irradiation on tumor reoxygenation as well as on subsequent HIF-1 activation.[8] The HIF-1-mediated promoter with eight copies of HRE has also been used to develop a novel PET imaging system.[37] In both cases, however, assessment in real-time seemed to be difficult,

because the reporter proteins were so stable[33] that some of them may have remained in the cells after reoxygenation. The reason why we choose d2EGFP rather than the other GFP derivatives was the short half-life of the protein, which is caused by the MODC domain fused in it.[33] In fact, we were able to demonstrate that d2EGFP fluorescence has a more rapid turnover than that of EGFP (Fig. 2F). Moreover, when we treated the cells with cyclohexamide just after the hypoxic treatment and just before reoxygenation, the d2EGFP fluorescence disappeared within 2 hours (data not shown). This MODC activity enabled us to assess HIF-1 activity in solid tumors in real-time.

Be11/CMV-d2EGFP showed homogeneous fluorescence in the whole tumor, while heterogeneous occurrence of green fluorescence was directly visualized in tumor xenografts inoculated with Be11/5HRE-d2EGFP cells. Our *in vitro* study enabled us to estimate to some extent the hypoxic status in the solid tumor. As Be11/5HRE-d2EGFP expressed detectable amounts of fluorescence in response to different hypoxic stimuli, e.g. 0.02% O_2 for 2 hours and <2% O_2 for 20 hours, we can assume that the fluorescent cells in the solid tumors were exposed to at least these conditions. At this time, however, an accurate assessment of tumor hypoxia with this method alone is not possible. For instance, it was difficult to distinguish the acute hypoxia from the chronic one. Moreover, we might not have visualized the acute hypoxia, but chronic one alone, because most gene expressions take a certain time. Therefore, combining our method with computer based image analysis and/or flow cytometry analysis can be expected to expand the efficacy and application of 5HRE-d2EGFP as an imaging system.

Immunohistochemical analysis clearly showed that the d2EGFP-expressing cells are located at a distance of about 100 μm from the tumor blood vessels, and the staining pattern is almost the same as the one obtained with anti-pimonidazole Ab. These results suggest that the 5HRE enhancer/promoter induces d2EGFP expressions in response to hypoxic stimuli in the solid tumor. However, more highly magnified images showed that more cells are stained with anti-GFP Ab than with anti-pimonidazole Ab in the boundary area between viable and necrotic regions (Fig. 4F and H). The quantitative analysis using NIH Image 1.63 software also clearly showed that there were certainly more GFP-expressing cells than pimonidazole-positive cells. Although these results might have been caused simply by the different sensitivities of the Abs, it is also possible that the HIF-1 activity is up-regulated by another regulatory pathway independent of hypoxia. The up-regulation of HIF-1α activity has been observed even under normoxic conditions in renal carcinoma cells, in which the von Hippel-Lindau tumor suppressor gene had lost its function.[38] Furthermore, HIF-1 activity increases when the PI3K/AKT signaling pathway is activated.[30] Regardless of the HIF-1-activating mechanisms, the 5HRE-d2EGFP system can reflect the HIF-1 activity, so that this system can be used for monitoring HIF-1 activity in real-time *in vivo*.

It has been reported that HIF-2 as well as HIF-1 regulates gene expression of VEGF, glycolytic enzymes and other HRE-driven genes in response to hypoxia.[39] Although HIF-2 plays some important roles in physiological stress response, the details of its mechanism and how it differs from that of the HIF-1 pathway remain unknown. To examine whether the 5HRE enhancer/promoter system is regulated by HIF-2 activity, too, we assessed its hypoxia responsiveness by using a squamous cell carcinoma cell line, in which the HIF-1α gene was mutated, and found evidence of the HIF-2-dependency of the 5HRE system. (in preparation). These findings indicate that this monitoring method can be used to analyze details of the activities of the HIF family *in vivo*. Moreover, this method can be expected to contribute to the development of HIFs-targeting drugs,[28] such as YC-1[40] and TOP3.[6,35,41]

ACKNOWLEDGEMENTS

We are grateful to Drs. N. Oya (Kumamoto University, Kumamoto, Japan) and S. Kizaka-Kondoh (Kyoto University, Kyoto, Japan) for discussion, and A. Morinibu for skilled technical assistance. This work was supported by research grants from the Ministry of Education, Science, Sports, and culture of Japan.

REFERENCES

1. Dang, C.V. and Semenza, G. L. (1999) Oncogenic alterations of metabolism. Trends Biochem. Sci. **24**: 68–72.
2. Vaupel, P., Kallinowski, F. and Okunieff, P. (1989) Blood flow, oxygen and nutrient supply, and metabolic microenvironment of human tumors: a review. Cancer Res. **49**: 6449–6465
3. Forsythe, J. A., Jiang, B. H., Iyer, N. V., Agani, F., Leung, S. W., Koos, R. D. and Semenza, G. L. (1996) Activation of vascular endothelial growth factor gene transcription by hypoxia-inducible factor 1. Mol. Cell Biol. **16**: 4604–4613.
4. Semenza, G. L., Roth, P. H., Fang, H. M. and Wang, G. L. (1994) Transcriptional regulation of genes encoding glycolytic enzymes by hypoxia-inducible factor 1. J. Biol. Chem. **269**: 23757–23763.
5. Zhong, H., De Marzo, A. M., Laughner, E., Lim, M., Hilton, D. A., Zagzag, D., Buechler, P., Isaacs, W. B., Semenza, G. L. and Simons, J. W. (1999) Overexpression of hypoxia-inducible factor 1alpha in common human cancers and their metastases. Cancer Res. **59**: 5830–5835.
6. Kizaka-Kondoh, S., Inoue, M., Harada, H. and Hiraoka, M. (2003) Tumor hypoxia: A target for selective cancer therapy. Cancer Sci. 94, 1021–1028.
7. Brown, J. M. (1999) The hypoxic cell: a target for selective cancer therapy--eighteenth Bruce F. Cain Memorial Award lecture. Cancer Res. **59**: 5863–5870.
8. Moeller, B. J., Cao, Y., Li, C. Y. and Dewhirst, M. W. (2004)

Radiation activates HIF-1 to regulate vascular radiosensitivity in tumors: role of reoxygenation, free radicals, and stress granules. Cancer Cell. **5**: 429–441.
9. Birner, P., Gatterbauer, B., Oberhuber, G., Schindl, M., Rossler, K., Prodinger, A., Budka, H. and Hainfellner, J. A. (2001) Expression of hypoxia-inducible factor-1 alpha in oligodendrogliomas: its impact on prognosis and on neoangiogenesis. Cancer. **92**: 165–171.
10. Schindl, M., Schoppmann, S. F., Samonigg, H., Hausmaninger, H., Kwasny, W., Gnant, M., Jakesz, R., Kubista, E., Birner, P. and Oberhuber, G.; Austrian Breast and Colorectal Cancer Study Group. (2002) Overexpression of hypoxia-inducible factor 1alpha is associated with an unfavorable prognosis in lymph node-positive breast cancer. Clin. Cancer Res. **8**: 1831–1837.
11. Bos, R., van der Groep, P., Greijer, A. E., Shvarts, A., Meijer, S., Pinedo, H. M., Semenza, G. L., van Diest, P. J. and van der Wall, E. (2003) Levels of hypoxia-inducible factor-1alpha independently predict prognosis in patients with lymph node negative breast carcinoma. Cancer. **97**: 1573–1581.
12. Birner, P., Schindl, M., Obermair, A., Plank, C., Breitenecker, G. and Oberhuber, G. (2000) Overexpression of hypoxia-inducible factor 1alpha is a marker for an unfavorable prognosis in early-stage invasive cervical cancer. Cancer Res. **60**: 4693–4696.
13. Aebersold, D. M., Burri, P., Beer, K. T., Laissue, J., Djonov, V., Greiner, R. H. and Semenza, G. L. (2001) Expression of hypoxia-inducible factor-1alpha: a novel predictive and prognostic parameter in the radiotherapy of oropharyngeal cancer. Cancer Res. **61**: 2911–2916.
14. Birner, P., Schindl, M., Obermair, A., Breitenecker, G. and Oberhuber, G. (2001) Expression of hypoxia-inducible factor 1alpha in epithelial ovarian tumors: its impact on prognosis and on response to chemotherapy. Clin. Cancer Res. **7**: 1661–1668.
15. Wang, G. L., Jiang, B. H., Rue, E. A. and Semenza, G. L. (1995) Hypoxia-inducible factor 1 is a basic-helix-loop-helix-PAS heterodimer regulated by cellular O2 tension. Proc. Natl. Acad. Sci. U S A. **92**: 5510–5514.
16. Kallio, P. J., Pongratz, I., Gradin, K., McGuire, J. and Poellinger, L. (1997) Activation of hypoxia-inducible factor 1alpha: posttranscriptional regulation and conformational change by recruitment of the Arnt transcription factor. Proc. Natl. Acad. Sci. U S A. **94**: 5667–5672.
17. Jaakkola, P., Mole, D. R., Tian, Y. M., Wilson, M. I., Gielbert, J., Gaskell, S. J., Kriegsheim, A. v., Hebestreit, H. F., Mukherji, M., Schofield, C. J., Maxwell, P. H., Pugh, C. W. and Ratcliffe, P. J. (2001) Targeting of HIF-alpha to the von Hippel-Lindau ubiquitylation complex by O2-regulated prolyl hydroxylation. Science. **292**: 468–472.
18. Semenza, G. L. (2001) HIF-1, O(2), and the 3 PHDs: how animal cells signal hypoxia to the nucleus. Cell. **107**: 1–3.
19. Wang, G. L. and Semenza, G. L. (1993) General involvement of hypoxia-inducible factor 1 in transcriptional response to hypoxia. Proc. Natl. Acad. Sci. U S A. **90**: 4304–4308.
20. Norris, M. L. and Millhorn, D. E. (1995) Hypoxia-induced protein binding to O2-responsive sequences on the tyrosine hydroxylase gene. J. Biol. Chem. **270**: 23774–23779.
21. Shibata, T., Akiyama, N., Noda, M., Sasai, K. and Hiraoka, M. (1998) Enhancement of gene expression under hypoxic conditions using fragments of the human vascular endothelial growth factor and the erythropoietin genes. Int. J. Radiat. Oncol. Biol. Phys. **42**: 913–916.
22. Shibata, T., Giaccia, A. J. and Brown, J. M. (2000) Development of a hypoxia-responsive vector for tumor-specific gene therapy. Gene Ther. **7**: 493–498.
23. Aboagye, E. O., Lewis, A. D., Johnson, A., Workman, P., Tracy, M. and Huxham, I. M. (1995) The novel fluorinated 2-nitroimidazole hypoxia probe SR-4554: reductive metabolism and semiquantitative localisation in human ovarian cancer multicellular spheroids as measured by electron energy loss spectroscopic analysis. Br. J. Cancer. **72**: 312–318.
24. Seddon, B. M., Payne, G. S., Simmons, L., Ruddle, R., Grimshaw, R., Tan, S., Turner, A., Raynaud, F., Halbert, G., Leach, M. O., Judson, I. and Workman, P. (2003) A phase I study of SR-4554 via intravenous administration for noninvasive investigation of tumor hypoxia by magnetic resonance spectroscopy in patients with malignancy. Clin. Cancer Res. **9**: 5101–5112.
25. Koch, C. J and Evans, S. M. (2003) Non-invasive PET and SPECT imaging of tissue hypoxia using isotopically labeled 2-nitroimidazoles. Adv. Exp. Med. Biol. **510**: 285–292.
26. Durand, R. E. and Raleigh, J. A. (1998) Identification of nonproliferating but viable hypoxic tumor cells *in vivo*. Cancer Res. **58**: 3547–3550.
27. Nordsmark, M., Loncaster, J., Aquino-Parsons, C., Chou, S. C., Ladekarl, M., Havsteen, H., Lindegaard, J. C., Davidson, S. E., Varia, M., West, C., Hunter, R., Overgaard, J. and Raleigh, J. A. (2003) Measurements of hypoxia using pimonidazole and polarographic oxygen-sensitive electrodes in human cervix carcinomas. Radiother. Oncol. **67**: 35–44.
28. Semenza, G. L. (2003) Targeting HIF-1 for cancer therapy. Nat. Rev. Cancer. **3**: 721–32.
29. Laughner, E., Taghavi, P., Chiles, K., Mahon, P. C. and Semenza, G. L. (2001) HER2 (neu) signaling increases the rate of hypoxia-inducible factor 1alpha (HIF-1alpha) synthesis: novel mechanism for HIF-1-mediated vascular endothelial growth factor expression. Mol. Cell. Biol. **21**: 3995–4004.
30. Zhong, H., Chiles, K., Feldser, D., Laughner, E., Hanrahan, C., Georgescu, M. M., Simons, J. W. and Semenza, G. L. (2000) Modulation of hypoxia-inducible factor 1alpha expression by the epidermal growth factor/phosphatidylinositol 3-kinase/PTEN/AKT/FRAP pathway in human prostate cancer cells: implications for tumor angiogenesis and therapeutics. Cancer Res. **60**: 1541–1545.
31. Fukuda, R., Hirota, K., Fan, F., Jung, Y. D., Ellis, L. M. and Semenza, G. L. (2002) Insulin-like growth factor 1 induces hypoxia-inducible factor 1-mediated vascular endothelial growth factor expression, which is dependent on MAP kinase and phosphatidylinositol 3-kinase signaling in colon cancer cells. J. Biol. Chem. **277**: 38205–38211.
32. Maxwell, P. H., Wiesener, M. S., Chang, G. W., Clifford, S. C., Vaux, E. C., Cockman, M. E., Wykoff, C. C., Pugh, C. W., Maher, E. R. and Ratcliffe, P. J. (1999) The tumour suppressor protein VHL targets hypoxia-inducible factors for oxygen-dependent proteolysis. Nature. **399**: 271–275.

33. Li, X., Zhao, X., Fang, Y., Jiang, X., Duong, T., Fan, C., Huang, C. C. and Kain, S. R. (1998) Generation of destabilized green fluorescent protein as a transcription reporter. J. Biol. Chem. **273**: 34970–34975.
34. Oya, N., Zolzer, F., Werner, F. and Streffer, C. (2003) Effects of serum starvation on radiosensitivity, proliferation and apoptosis in four human tumor cell lines with different p53 status. Strahlenther Onkol. **179**: 99–106.
35. Harada, H., Hiraoka, M. and Kizaka-Kondoh, S. (2002) Antitumor effect of TAT-oxygen-dependent degradation-caspase-3 fusion protein specifically stabilized and activated in hypoxic tumor cells. Cancer Res. **62**: 2013–2018.
36. Heim, R., Prasher, D. C. and Tsien RY. (1994) Wavelength mutations and posttranslational autoxidation of green fluorescent protein. Proc. Natl. Acad. Sci. U S A. **91**:12501–12504.
37. Serganova, I., Doubrovin, M., Vider, J., Ponomarev, V., Soghomonyan, S., Beresten, T., Ageyeva, L., Serganov, A., Cai, S., Balatoni, J., Blasberg, R. and Gelovani, J. (2004) Molecular imaging of temporal dynamics and spatial heterogeneity of hypoxia-inducible factor-1 signal transduction activity in tumors in living mice. Cancer Res. **64**: 6101–6108.
38. Krieg, M., Haas, R., Brauch, H., Acker, T., Flamme, I. and Plate, K. H. (2000) Up-regulation of hypoxia-inducible factors HIF-1alpha and HIF-2alpha under normoxic conditions in renal carcinoma cells by von Hippel-Lindau tumor suppressor gene loss of function. Oncogene. **19**: 5435–5443.
39. Ema, M., Taya, S., Yokotani, N., Sogawa, K., Matsuda, Y. and Fujii-Kuriyama, Y. (1997) A novel bHLH-PAS factor with close sequence similarity to hypoxia-inducible factor 1alpha regulates the VEGF expression and is potentially involved in lung and vascular development. Proc. Natl. Acad. Sci. U S A. **94**: 4273–4278.
40. Yeo, E. J., Chun, Y. S., Cho, Y. S., Kim, J., Lee, J. C., Kim, M. S. and Park, J. W. (2003) YC-1: a potential anticancer drug targeting hypoxia-inducible factor 1. J. Natl. Cancer Inst. **95**: 516–525.
41. Inoue, M., Mukai, M., Hamanaka, Y., Tatsuta, M., Hiraoka, M. and Kizaka-Kondoh, S. (2004) Targeting hypoxic cancer cells with a protein prodrug is effective in experimental malignant ascites. Int. J. Oncol. **25**: 713–720.

Received on November 19, 2004
1st Revision received on December 22, 2004
Accepted on December 22, 2004

RESEARCH ARTICLE

Molecular Imaging • Vol. 4, No. 3, July 2005, pp. 182–193

Optical Imaging of Tumor Hypoxia and Evaluation of Efficacy of a Hypoxia-Targeting Drug in Living Animals

Hiroshi Harada, Shinae Kizaka-Kondoh, and Masahiro Hiraoka

Kyoto University Graduate School of Medicine, Japan

Abstract

Solid tumors containing more hypoxic regions show a more malignant phenotype by increasing the expression of genes encoding angiogenic and metastatic factors. Hypoxia-inducible factor-1 (HIF-1) is a master transcriptional activator of such genes, and thus, imaging and targeting hypoxic tumor cells where HIF-1 is active are important in cancer therapy. In the present study, HIF-1 activity was monitored via an optical in vivo imaging system by using a luciferase reporter gene under the regulation of an artificial HIF-1-dependent promoter, 5HRE. To monitor tumor hypoxia, we isolated a stable reporter-transfectant, HeLa/5HRE-Luc, which expressed more than 100-fold luciferase in response to hypoxic stress, and observed bioluminescence from its xenografts. Immunohistochemical analysis of the xenografts with a hypoxia marker, pimonidazole, confirmed that the luciferase-expressing cells were hypoxic. Evaluation of the efficacy of a hypoxia-targeting prodrug, TOP3, using this optical imaging system revealed that hypoxic cells were significantly diminished by TOP3 treatment. Immunohistochemical analysis of the TOP3-treated xenografts confirmed that hypoxic cells underwent apoptosis and were removed after TOP3 treatment. These results demonstrate that this model system using the 5HRE-luciferase reporter construct provides qualitative information (hypoxic status) of solid tumors and enables one to conveniently evaluate the efficacy of cancer therapy on hypoxia in malignant solid tumors. *Mol Imaging* (2005) **4**, 182–193.

Keywords: Hypoxia-inducible factor-1 (HIF-1), tumor hypoxia, hypoxia response element (HRE), luciferase bioluminescence, optical imaging.

Introduction

An insufficient blood supply to a rapidly growing tumor leads to the presence of hypoxia, which is a well-known feature of solid tumors [1]. It is clinically important that insufficient tumor oxygenation affects the efficiency of chemotherapy and radiotherapy [2–4]. Moreover, hypoxic conditions increase the aggressiveness of tumor cells by inducing the expression of several genes related to proliferation, angiogenesis, invasion, and metastasis to aid survival in the severe tumor microenvironment [5–7]. Most of such genes contain a hypoxia responsive element (HRE), which is the binding site of hypoxia inducible factor-1 (HIF-1) [8], the master transcriptional regulator of cellular adaptive responses to hypoxic stress [5,9]. HIF-1 is a heterodimer that consists of an alpha subunit (HIF-1α) and the constitutively expressed beta subunit (HIF-1β). HIF-1α expression is regulated in an oxygen-dependent manner at the posttranslational level and is responsible for the regulation of HIF-1 activity [9]. In normoxia, HIF-1α is hydroxylated on the proline residues in the oxygen-dependent degradation domain (ODD) by prolyl hydroxylases [10,11]. The hydroxylated proline residues accelerate the interaction of HIF-1α protein with von Hippel–Lindau tumor suppressor protein, resulting in the rapid ubiquitination and subsequent degradation of HIF-1α [5,12–15].

HIF-1 as well as tumor hypoxia have been recognized as a crucial target for cancer therapy, therefore, strategies detecting and evaluating them are desired [5,16]. Recently, hypoxia-responsive promoters have been applied to develop hypoxia imaging and targeting strategies. HRE derived from vascular endothelial cell growth factor (VEGF) promoter [8] has been employed to establish the artificial hypoxia-responsive promoter. The promoters containing HRE in tandem significantly increase the gene expressions in response to hypoxic stress and successfully induce anti-tumor effects in vivo [17–22]. Above all, 5HRE promoter, which consists of five copies of HRE and human cytomegalovirus minimal promoter, enhances more than 500-fold transcription under the hypoxic conditions than under the aerobic conditions [19]. Green fluorescent protein [20,21] and a prodrug-activating enzyme [22] under the regulation of 5HRE promoter show the potential for tumor hypoxia-specific imaging and targeting, respectively. We have

Abbreviations: HE, hematoxylin–eosin; HIF, hypoxia-inducible factor; HIV-1, human immunodeficiency virus type-1; HRE, hypoxia response element; ODD, oxygen-dependent degradation; PTD, protein transduction domain; siRNA, small interfering RNA; TOP3, tat-ODD-procaspase-3; TUNEL, TdT-mediated dUTP nick end labelling; VEGF, vascular endothelial growth factor.

Corresponding author: Shinae Kizaka-Kondoh, COE Formation for Genomic Analysis of Disease Model Animals with Multiple Genetic Alterations, Department of Radiation Oncology and Imaging-applied Therapy, Kyoto University Graduate School of Medicine, 54 Kawahara-cho, Shogoin, Sakyo-ku, Kyoto, 606-8507, Japan; e-mail: skondoh@kuhp.kyoto-u.ac.jp.

Received 31 January 2005; Received in revised form 24 March 2005; Accepted 3 May 2005.

developed a protein prodrug, TOP3 [23,24], which is composed of the protein transduction domain derived from human immunodeficiency virus-1 tat protein (HIV tat-PTD), a part of HIF-1α ODD domain and the dormant form of caspase-3, procaspase-3. HIV tat-PTD fusion proteins can be delivered to many different cells in the whole body in a concentration-dependent manner [25,26] and ODD fusion proteins can be specifically stabilized under hypoxic conditions [23]. Therefore, hypoxia-specific targeting of tumor cells has been accomplished by TOP3 in hypoxic ascites as well as in vitro [23,27].

In this report, we demonstrate that the imaging system using a 5HRE-luciferase reporter gene can efficiently detect and monitor tumor hypoxia where HIF-1 is active in living mice. By using this system, we successfully demonstrate that TOP3 certainly targets hypoxic tumor cells in solid tumors, indicating that this model system allows sensitive, real-time, and spatio-temporal analyses of tumor hypoxia in solid tumors and provides a useful method to evaluate the efficacy of a cancer therapy on hypoxia in malignant solid tumors.

Materials and Methods

Cell Cultures, Reagents, and Hypoxic Treatment

The human cervical epithelial adenocarcinoma cell line, HeLa, and the human pancreatic cancer cell line, CFPAC-1, were purchased from the American Type Culture Collection (#CCL-2 and #CRL-1918, respectively). HeLa cells were maintained in 5% FBS–Dulbecco's modified Eagle's medium, and CFPAC-1 cells were maintained in 10% FBS–Iscove's modified Dulbecco's medium (Nacalai Tesque, Kyoto, Japan). Both of the mediums were supplemented with penicillin (100 units/mL) and streptomycin (100 μg/mL). To create a hypoxic condition of <0.02% of oxygen tension, the cells were treated in a Bactron Anaerobic Chamber, BACLITE-1 (Sheldon Manufacturing, Cornelius, OR).

Preparation of Protein Prodrug

TOP3 was overexpressed in *Escherichia coli* and purified as described previously [23]. Purified TOP3 was dissolved in Tris–HCl buffer (pH 8.0) at a concentration of 1 mg/mL.

Plasmid DNA

To construct the pEF/Luc plasmid, which constitutively expresses luciferase under the control of EF-1α promoter [28], luciferase cDNA was amplified from pGL3 promoter vector (Promega, Madison, WI) by PCR using Luc-Bam-sense primer; AAGGATCCACCATGGAAGACGCCAAA and Luc-RV-anti primer; TTGATATCTTACACGGCGATCTTTCC. The PCR product was then digested with *Bam*HI and *Eco*RV and inserted between *Bam*HI and *Eco*RV recognition sites of pEF6/Myc-His B plasmid (Invitrogen, Carlsbad, CA). To construct the pEF/5HRE-Luc plasmid, the DNA fragment, which consists of 5HRE promoter and luciferase gene, was obtained by *Kpn*I and *Xba*I digestion of 5HRE-hCMVmp-Luc plasmid [19] and inserted between *Kpn*I and *Xba*I recognition sites of pEF/myc/cyto plasmid (Invitrogen).

Isolation of HeLa/EF-Luc and HeLa/5HRE-Luc Cells

To establish HeLa/EF-Luc and HeLa/5HRE-Luc cell clones, HeLa cells were transfected with pEF/Luc plasmid and pEF/5HRE-Luc plasmid, respectively, by calcium phosphate method using the Mammalian Transfection Kit (Stratagene, La Jolla, CA) and were selected by culturing for an additional 10 days in the culture medium containing 5 μg/mL of blasticidine S (Invitrogen) for HeLa/EF-Luc or 400 μg/mL of G418 (Nacalai Tesque) for HeLa/5HRE-Luc. Antibiotics-resistant colonies were isolated and established as clones. Representative clones were used here.

Luciferase Assay in vitro and Western Blot Analysis

HeLa/5HRE-Luc cells were seeded onto a 24-well dish (1×10^4 cells/well) and cultured under aerobic or hypoxic conditions for 0, 1, 2, 4, 8, and 16 hr. The cells were then washed with PBS and lyzed with 100 μL Passive Lysis Buffer (Promega) and 10 μL of the lysates were applied for the luciferase assay (Promega). For Western blot analysis, the cells were directly harvested in the 100 μL of 1× loading buffer [29] after the same hypoxic treatment as above, and 20 μL of them were electrophoresed on a 7.5% SDS–polyacrylamide gel and transferred onto PVDF membrane (Amersham Biosciences, Piscataway, NJ). HIF-1α protein was detected with monoclonal anti-HIF-1α antibody (BD Bioscience Pharmingen, San Diego, CA) and anti-mouse IgG horseradish peroxidase linked whole antibody (Amersham Bioscience) using the ECL-PLUS system (Amersham Bioscience) according to the manufacturer's instruction.

Real-time Monitoring of Luciferase Activity in vivo

Cell suspensions of HeLa/EF-Luc cells and HeLa/5HRE-Luc cells (1×10^6 cells/100 μL of PBS) were subcutaneously inoculated into the left and right hind legs of 6-week-old female nude mice (BALB/c *nu/nu*; Japan SLC, Hamamatsu, Japan), respectively. The mice were

used for each experiment 10 days after the implantation. For the in vivo imaging of bioluminescence, the tumor-bearing mice were intravenously injected with 100 μL of D-luciferin solution (10 mg/mL in PBS; Promega). And exactly 15 min later, the mice were applied to IVIS™-100 in vivo Imaging System (Xenogen, Alameda, CA) to measure the luciferase activity as the externally detected photon count. During imaging, the mice were kept on the imaging stage in the anesthetized condition with 2.5% of isoflurane gas in oxygen flow (1.5 L/min). Obtained images were analyzed by using Living Image 2.50—Igor Pro 4.09A software (Xenogen). Pixel intensities within the regions of interest were summed to yield integrated intensity of bioluminescence as photon counts. In all of the imaging experiments, reproducibility was confirmed by using 5 independent tumor-bearing mice, and representative images are shown.

Growth Delay Assay

The tumor mass of CFPAC-1 xenografts was measured with a caliper, and the tumor mass was calculated as $0.5 \times L \times W^2$. The tumor mass of HeLa/EF-Luc xenografts was measured as the externally detected photon counts. The tumor mass on each day was compared with the one on Day 0, to calculate the relative tumor mass.

Immunohistochemical Analysis

Pimonidazole hydrochloride (Natural Pharmacia International, Belmont, MA) was intraperitoneally injected into tumor-bearing mice (60 mg/kg) at 90 min before surgical excision of solid tumor in each experiment. The excised solid tumors were fixed in 10% formalin neutral buffer solution (pH = 7.4; Wako Pure Chemical Industries, Osaka, Japan) and embedded in paraffin.

To detect pimonidazole-binding and luciferase proteins, paraffin-embedded sections were treated with anti-pimonidazole (Natural Pharmacia International) and anti-luciferase (Promega) antibodies, respectively, and stained by indirect immunoperoxidase detection method (DakoCytomation, Carpinteria, CA). Counterstaining with hematoxylin was also conducted. Paraffin-embedded serial sections were also stained with hematoxylin–eosin (HE). To calculate the percentage of hypoxic regions, pimonidazole-positive areas were quantified using NIH Image 1.63 software (NIH, Bethesda, MD) and compared with the one of whole tumor. This analysis was conducted in a double-blind fashion.

For the detection of apoptotic cells, the paraffin-embedded sections were stained with ApopTag Fluorescein In Situ Apoptosis Detection Kit (Chemicon International, Temecula, CA), according to the manufacturer's instruction.

Statistical Analysis

Data are expressed as means ± *SD*. Statistical significance of differences was determined by the paired two-tailed Student's *t* test. Differences were considered statistically significant for $p < .05$.

Results

HIF-1-dependent Luciferase Activity in HeLa/5HRE-Luc Cells

To assess the HIF-1 activity in solid tumors, we took advantage of the HIF-1-mediated gene expression. We isolated a stable HeLa clone (HeLa/5HRE-Luc) after transfection with 5HRE-hCMVmp-Luciferase reporter gene [19], which was reported to induce luciferase expression in response to hypoxic stress. When HeLa/5HRE-Luc cells were cultured under hypoxic conditions, their luciferase activity was increased 100-fold more than the one cultured under aerobic conditions (Figure 1A). HIF-1α proteins were gradually stabilized over the hypoxic treatment periods (Figure 1B). These data indicate

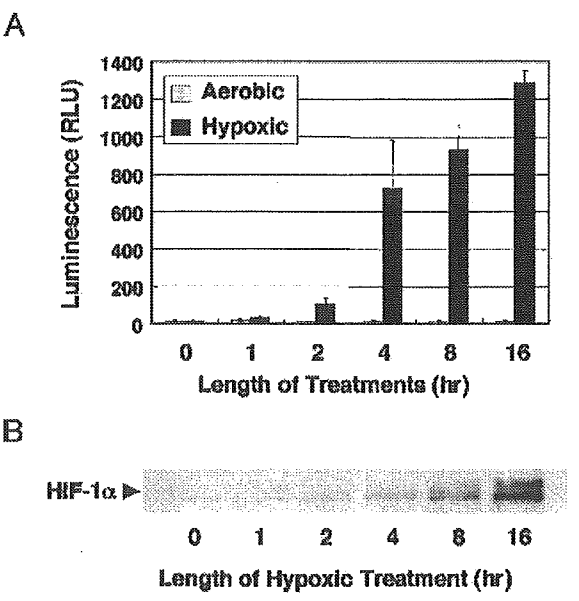

Figure 1. *HIF-1-dependent luciferase activity in HeLa/5HRE-Luc cells. (A) HeLa/5HRE-Luc cells were treated under aerobic or hypoxic conditions for the indicated time and their luciferase activities were measured and luminescence (RLU) is shown in the figure. The results are the mean ± SD, n = 3. (B) HeLa/5HRE-Luc cells were treated under hypoxic conditions for the indicated time and HIF-1α protein expression was analyzed by Western blotting.*

that the HeLa/5HRE-Luc cells can be employed to monitor the oxygen-dependent HIF-1 activity.

Optical Imaging of HIF-1 Activity in Tumor Xenograft

Optical in vivo imaging systems enable us to detect tumor cells in the same animals repeatedly [30], and thus, we can monitor the change of luciferase activity in the same tumor xenografts by measuring bioluminescence throughout the experiment period. We first examined HeLa/5HRE-Luc xenografts by immunohistochemical analysis if luciferase expression was corresponding with hypoxic microenvironment in them. The presence of hypoxic cells in solid tumors was assessed by using a bioreductive hypoxia marker, pimonidazole hydrochloride [31]. The regions detected with anti-luciferase antibody (Figure 2Aa; dark brown) were almost identical to the pimonidazole-positive regions (Figure 2Ab; dark brown), and both were located at the boundary areas between viable (Figure 2Ac; V) and necrotic regions (Figure 2Ac; N), indicating that the cells expressing luciferase were certainly hypoxic. The bioluminescence from the HeLa/5HRE-Luc tumor xenografts was externally monitored by optical in vivo imaging system (Figure 2Ba; right hind leg).

To confirm that the intensity of bioluminescence from HeLa/5HRE-Luc xenografts reflects hypoxic status in the xenografts, we reduced the blood flow to the HeLa/5HRE-Luc xenografts by ligaturing the tumor-bearing right legs and examined the xenografts via an optical in vivo imaging system at the indicated time (Figure 2Ba–Bd). HeLa/EF-Luc tumor xenografts, in which luciferase was constitutively expressed, were set in the left hind legs and were untreated during the experiment as an internal control for the imaging procedure. The bioluminescence from the ligatured HeLa/5HRE-Luc xenografts increased over time (Figure 2Ba–Bd), whereas changes in bioluminescent intensity were hardly observed without ligature (Figure 2Be–Bh). To examine whether the increase in bioluminescence was dependent on the 5HRE promoter, we conducted same experiments using the mice with HeLa/EF-Luc xenografts in both legs. The bioluminescence intensity from the HeLa/EF-Luc xenografts was not influenced by the ligaturing (data not shown). Each experiment was conducted by using 5 independent tumor-bearing mice to confirm reproducibility, and representative images are shown in the figure. These results indicate that the increase of bioluminescence from ligatured HeLa/5HRE-Luc xenograft reflected the increase of hypoxic regions because of poor blood supply and suggest that the 5HRE-luciferase reporter system can be used to monitor tumor hypoxia in solid tumors via in vivo imaging system.

Evaluation of Hypoxia-targeting Efficacy of TOP3 with the Optical Imaging Method

We recently developed an anti-tumor protein prodrug, TOP3, which is composed of HIV-1 tat-PTD, a part of HIF-1α ODD domain and procaspase-3 (Figure 3). Because Tat-PTD ensures the in vivo delivery of fusion protein into a variety of different cells in a rapid and concentration-dependent manner [25,26], and the ODD domain facilitates the specific stabilization of fusion protein under hypoxic conditions [23], tat-ODD fusion protein, whose stability is regulated through the same ODD-dependent mechanism as HIF-1α protein, is accumulated in the hypoxic tumor cells in vivo [23,27]. Accumulated TOP3 is subsequently cleaved by endogenous caspases, which are activated to some extent by hypoxic stress, and increases active caspase-3, resulting in hypoxia-specific cell death in hypoxic ascites as well as in vitro [23,27]. Although TOP3 did reduce the volume of solid tumors, it was not clear if TOP3 targeted hypoxic tumor cells in solid tumors. By using this imaging method, we can monitor hypoxic tumor cells over TOP3 treatment period, and thus, we can clarify the TOP3 effect on solid tumors.

TOP3 was intraperitoneally injected into nude mice (n = 5) with a HeLa/5HRE-Luc xenograft in the right hind leg and with a HeLa/EF-Luc xenograft in the left hind leg three times in 5-day intervals. The bioluminescent signals from both xenografts were monitored via the in vivo imaging system and relative photon counts and representative images are shown (Figure 4A–C). Because the photon count corresponds to tumor mass when the luciferase is constitutively expressed in the tumor cells [30], the effect of TOP3 on whole tumor mass was measured as the bioluminescence from the HeLa/EF-Luc xenograft in the left hind leg. On the other hand, the effect of TOP3 on hypoxic tumor cells was assessed as the bioluminescence from the HeLa/5HRE-Luc xenograft in the right hind leg. The bioluminescent signals from both HeLa/EF-Luc and HeLa/5HRE-Luc xenografts of buffer-treated mice increased over the observation periods (Figure 4A, B, and Ca–Cc). In the buffer-treated mice, the increase in the bioluminescence from hypoxic regions was more than 22-fold (Figure 4B) during the period, in which the whole tumor mass increased about 16-fold (Figure 4A), indicating that hypoxic regions gradually increased as the tumor volume increased. On the other hand, the bioluminescence from hypoxic regions of the TOP3-treated mice was

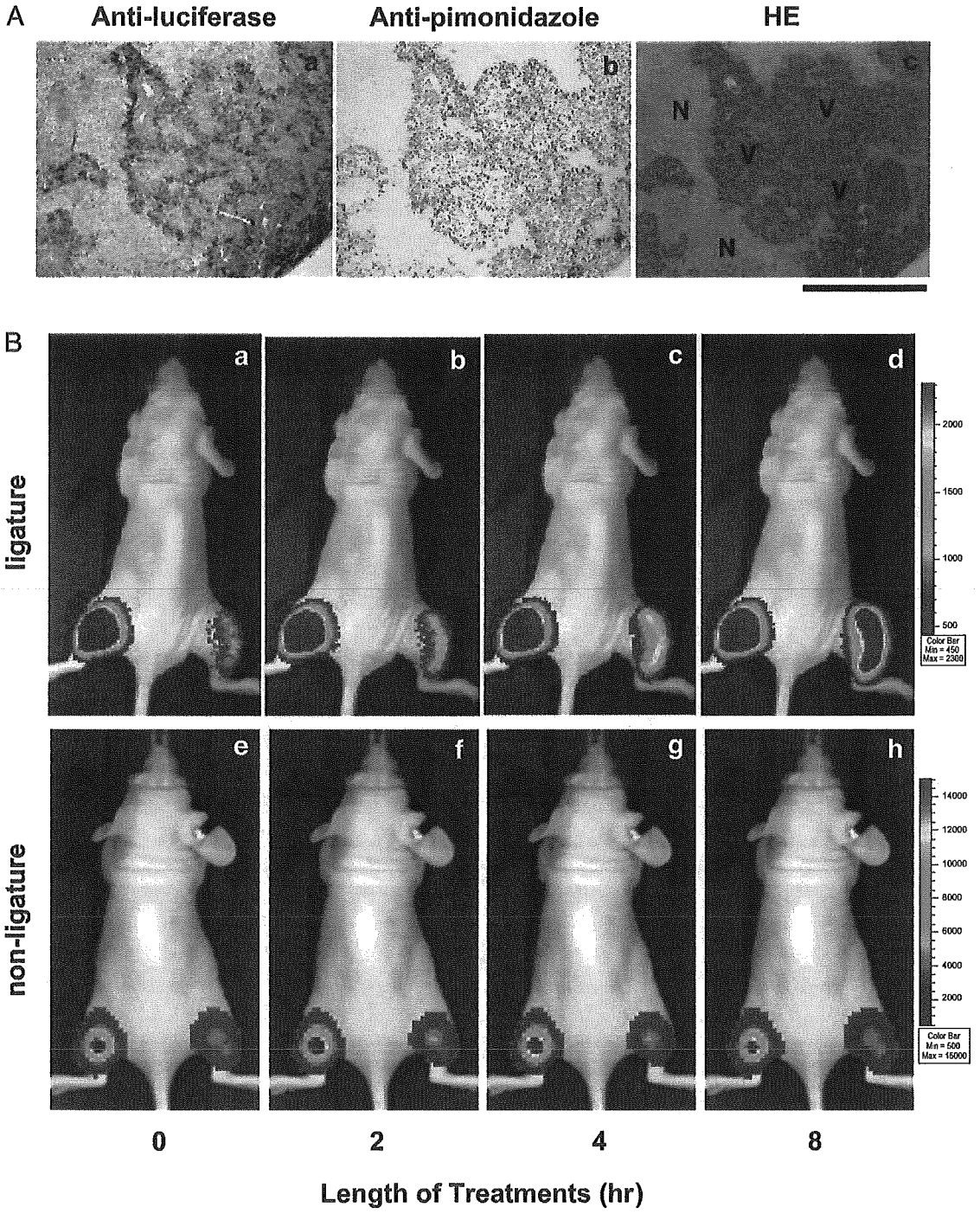

Figure 2. *Optical imaging of HIF-1 activity in HeLa/5HRE-Luc tumor xenografts. (A) Serial sections of HeLa/5HRE-Luc xenograft were subjected to immunohistochemical analysis with anti-luciferase antibody (a) and anti-pimonidazole antibody (b), and to HE staining (c). N = necrotic tumor tissue; V = well-oxygenated viable tumor tissue. (B) HeLa/EF-Luc cells and HeLa/5HRE-Luc cells were subcutaneously inoculated into the left and right hind legs, respectively (a–h). Blood flow to the HeLa/5HRE-Luc xenograft was decreased by ligaturing the right hind leg (a–d). During the ligaturing treatment, change in bioluminescence was sequentially monitored in the same mouse just after (a), 2 hours after (b), 4 hours after (c), and 8 hours after (d) the beginning of ligaturing. As a control, the bioluminescence was sequentially monitored without the ligature at the same time course (e–h). HeLa/EF-Luc xenograft in the left leg was left untreated as an internal control. During the experiment, mice were kept exposed to anesthesia with 2.5% of isoflurane gas in oxygen flow (1.5 L/min) and put on the imaging stage.*

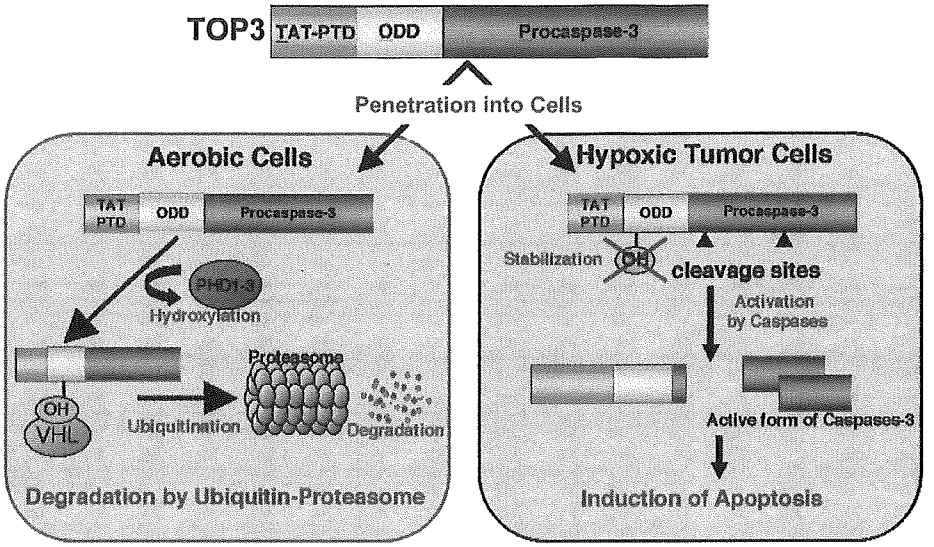

Figure 3. *Oxygen-dependent degradation and hypoxia-specific activation of TOP3. In well-oxygenated cells, TOP3 will be degraded through the same ubiquitin–proteasome system as HIF-1α protein (for details, see Ref. [16]). In hypoxic tumor cells, TOP3 are stabilized, and upstream caspases are activated to some extent by hypoxic stress, and therefore, TOP3 will be cleaved to generate an active caspase-3, inducing apoptotic cell death.*

minimized on Day 3 after the first administration and was continuously suppressed during the treatment period (Figure 4B and Cd–Cf: right legs), in which whole tumor mass increased about 9-fold (Figure 4A). These data clearly demonstrate the hypoxia-targeting effect of TOP3 in solid tumors.

Specific Targeting of Hypoxic Tumor Cells by TOP3 in vivo

To investigate whether the suppressed bioluminescence in TOP3-treated xenografts were the consequence of the reduction of hypoxic/HIF-1-activating cells in solid tumors, we investigated the sections of TOP3-treated xenografts by immunohistochemical analysis. To avoid the influence of luciferase expression, CFPAC-1 xenografts were examined with the same experimental time frame as HeLa/5HRE-Luc xenografts. First of all, we confirmed that the growth of CFPAC-1 xenografts was comparatively suppressed during TOP3 treatment (Figure 5A). The growth of TOP3-treated tumors was suppressed during the sequential TOP3 treatment, but accelerated thereafter (>Day 15); the slope of the growth curve of buffer-treated tumors was 0.211. The slope of the TOP3-treated tumor (from Day 0 to Day 15) was 0.087, but it reverted to a similar slope to that of the untreated tumor after Day 15 (0.225). Tumor growth doubling time (TGDT) clearly shows a growth delay of TOP3-treated tumors (Table 1; $p < .05$). TOP3 treatment decreased the growing speed of the CFPAC-1 tumor to almost one-third of the untreated ones.

The tumors were surgically excised 5, 24, and 48 hr after TOP3 administration, and were embedded in paraffin for HE staining and for immunohistochemical analysis with anti-pimonidazole antibody. We repeated the above staining with three to four independent tumors for each group. The percentage of pimonidazole-positive cells (dark brown) in a whole solid tumor represents the percentage of hypoxic regions (Figure 5B). Hypoxic regions in the 48-hr samples from TOP3-treated xenografts were significantly reduced compared with the ones in buffer-treated xenografts ($p < .01$). The staining pattern of serial sections from the 5-hr samples was basically the same between TOP3-treated and buffer-treated xenografts, whereas the patterns of 24- and 48-hr samples from TOP3-treated xenografts

Figure 4. *Evaluation of the efficacy of TOP3 via an optical in vivo imaging system. Tumor-bearing mice with HeLa/EF-Luc cells (left hind leg) and HeLa/5HRE-Luc cells (right hind leg) were intraperitoneally injected with Tris–HCl buffer (pH 8.0) or TOP3 (20 mg/kg) on Days 0, 5, and 10. (A) To calculate the relative tumor mass during the buffer or TOP3 treatments, the bioluminescence (photons/sec/ROI) from HeLa/EF-Luc tumor xenograft in the left hind leg on each day was divided by the one on Day 0 and shown as relative photon counts. The results are the mean of 5 independent tumor-bearing mice ± SD for each group. *$p < .05$. (B) To calculate the relative hypoxic regions during the buffer or TOP3 treatments, the bioluminescence (photons/sec/ROI) from HeLa/5HRE-Luc tumor xenograft in the right leg on each day was divided by the one on Day 0 and shown as relative photon counts. The results are the mean of 5 independent tumor-bearing mice ± SD for each group. *$p < .05$. **$p < .01$. (C) The bioluminescence was externally monitored by IVIS imaging system to analyze the effects of the TOP3 treatments on the whole tumor mass (see left hind leg) and on the hypoxic regions (see right hind leg). Representative images just after (a and d), 3 days after (b and e), and 13 days after (c and f) initial TOP3 injection are shown.*

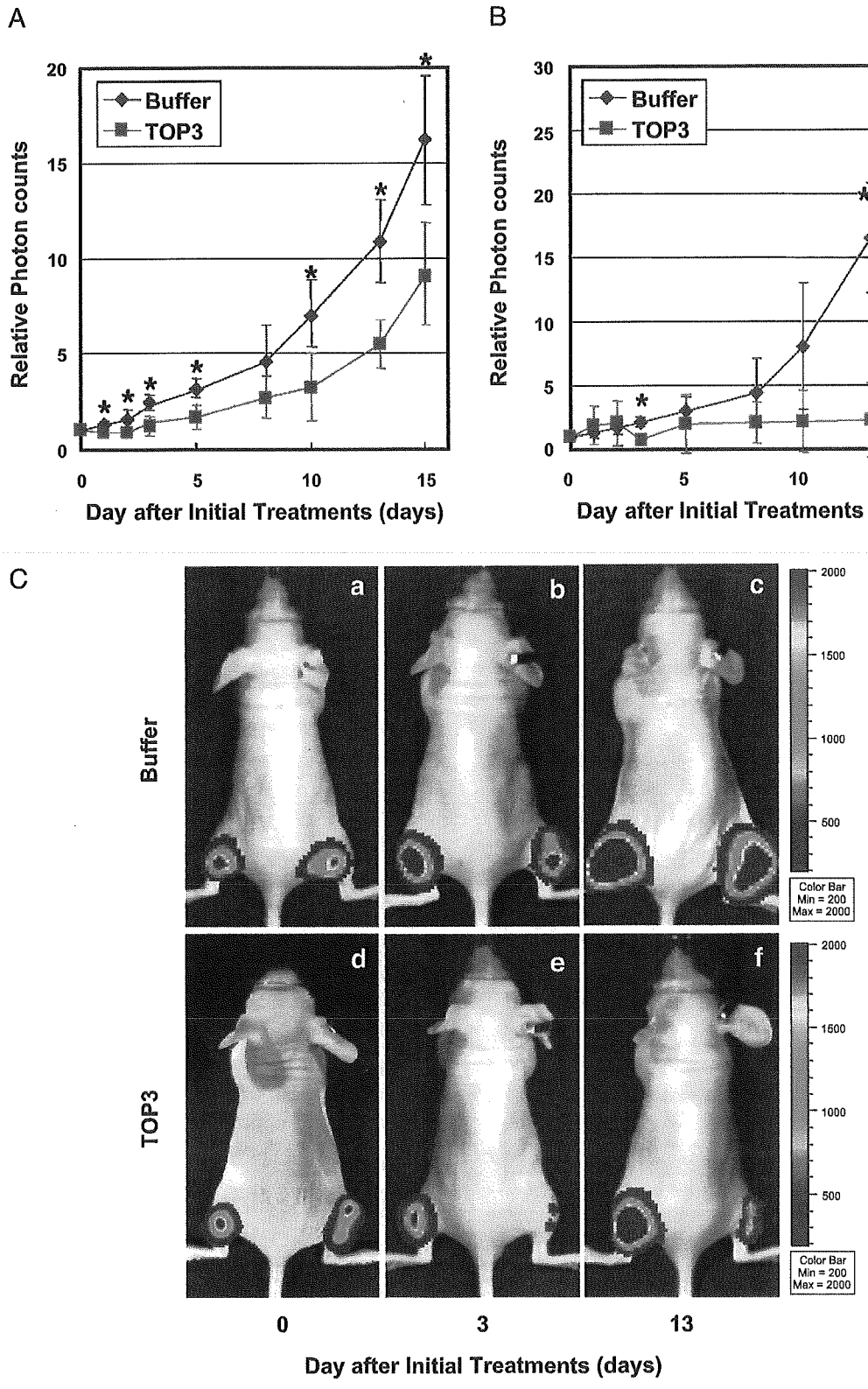
A
B
C
Buffer
TOP3
Relative Photon counts
Day after Initial Treatments (days)
a
b
c
d
e
f
2000
1500
1000
500
Color Bar
Min = 200
Max = 2000
0
3
13

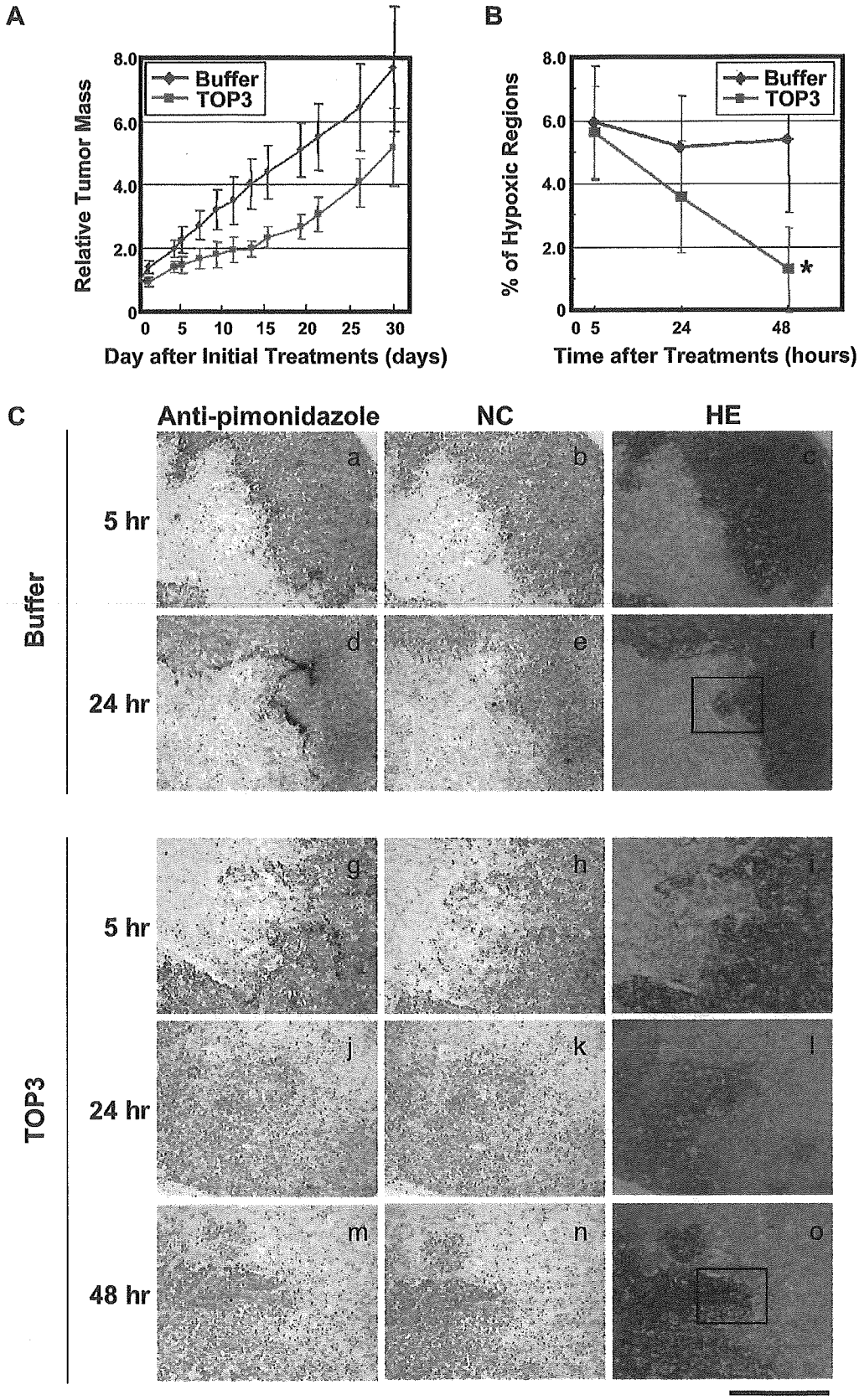
A
Relative Tumor Mass
Buffer
TOP3
8.0
6.0
4.0
2.0
0
0 5 10 15 20 25 30
Day after Initial Treatments (days)
B
% of Hypoxic Regions
Buffer
TOP3
8.0
6.0
4.0
2.0
0
0 5 24 48
*
Time after Treatments (hours)
C
Anti-pimonidazole
NC
HE
Buffer
5 hr
24 hr
TOP3
5 hr
24 hr
48 hr
a
b
c
d
e
f
g
h
i
j
k
l
m
n
o

were totally different from those of buffer-treated ones (Figure 5C). The pimonidazole-positive cells were gradually decreased in the TOP3-treated sections (Figure 5Cg, Cj, and Cm). Higher magnified images clearly show that the boundary areas between viable regions and necrotic regions, which corresponded to pimonidazole-positive cells in buffer-treated xenografts, were empty spaces in the TOP3-treated samples (Figure 6D–F). To investigate the status of the hypoxic tumor cells between 5 and 24 hr after TOP3 treatment, we examined xenografts with TαT-mediated αUTP nick end labelling (TUNEL) at 12 hr after TOP3 treatment. Much more TUNEL-positive green fluorescence was detected around the boundary area between viable and necrotic cells in the TOP3-treated xenograft than in the buffer-treated xenograft (compare Figure 7A with Figure 7D). These data indicate that TOP3 induces apoptosis in hypoxic tumor cells of the boundary regions and efficiently eliminates these cells.

Table 1. Statistical Analysis of TGDT

Treatment	HeLa/5HRE-Luc (days ± SD)	CFPAC-1 (days ± SD)
Buffer	3.2 ± 1.2	4.8 ± 2.3
TOP3	7.6 ± 2.4*	12.6 ± 5.4*

TGDT was calculated as the mean of the days on which relative tumor mass of each tumor reached to two fold of the one on Day 0. Data were based on the results obtained by using HeLa/5HRE-Luc cells (n = 5) and CFPAC-1 cells (n = 6) in Figures 4A and 5A, respectively.
*p < .05 (vs. buffer).

Discussion

Recent progress in optical imaging in vivo provides us with various information such as neoplastic cell growth [30], molecular localization [32], enzymatic reaction [33], and protein–protein interactions [34] in living animals. It also contributes towards collecting internal information without the sacrifice of animals. All of the results presented here demonstrate that the optical imaging method using 5HRE-luciferase reporter gene enables us to efficiently and easily monitor tumor hypoxia, where HIF-1 is active in living animals, and precisely evaluate the efficacy of anti-cancer therapies on tumor hypoxia.

HIF-1-dependent promoter has been used to monitor hypoxic status in tumors [20,21,35]. Their reporters were fluorescent proteins. Because permeability of bioluminescence in living animals is much better than fluorescence, a luciferase reporter system allowed sensitive, quantitative, real-time spatio-temporal analyses of the dynamics of neoplastic cell growth [30]. Because the quantitation of total photons from xenografts, in which tumor cells express luciferase gene under a constitutively active promoter, is an indicator of tumor burden [30], progressive tumor growth or regression could be monitored by repeated analyses of HeLa/EF-Luc xenografts at serial time points (Figure 4A and C, tumors in left legs). On the other hand, because the quantitation of total photons from HeLa/5HRE-Luc xenografts is an indicator of tumor hypoxia, qualitative information (hypoxic status) of solid tumors could be obtained by this model system (Figure 4B and C, tumors in right legs). When the growths of HeLa/EF-Luc and HeLa/5HRE-Luc xenografts were assessed with caliper, they were equally suppressed with TOP3 treatment in vivo (data not shown), indicating that both xenografts showed equal sensitivity to TOP3 treatment. These results further strengthen the argument that the decrease in photon counts from TOP3-treated HeLa/5HRE-Luc would reflect the decrease of tumor hypoxia in the xenografts (Figure 4B and C).

According to the previous report, the HIF-1α small interfering (si) RNA, but not the HIF-2α siRNA, suppresses hypoxia-dependent VEGF promoter activity in HeLa cells [36]. This suggests that the HRE from the VEGF promoter is exclusively dependent on HIF-1 activity in HeLa cells. Moreover, Western blot analysis confirmed that the up-regulation of luciferase activity was accompanied with the stabilization of HIF-1α protein in HeLa/5HRE-Luc cells (Figure 1). Because HIF-1 activity is closely associated with tumor hypoxia [37] and the HIF-1-induced expression of luciferase corresponds with hypoxic region in HeLa/5HRE-Luc xenografts (Figure 2A), bioluminescence from the xenografts should reflect the existence of tumor hypoxia where HIF-1 is active.

Figure 5. *Decrease in hypoxic/HIF-1-expressing cells in the TOP3-treated tumor xenografts. (A) CFPAC-1 tumor-bearing mice were intraperitoneally injected with buffer or TOP3 on Days 0, 5, and 10. To calculate the relative tumor mass, the tumor mass measured with caliper on each day was divided by the one on Day 0. Results are the mean of 6 independent tumor-bearing mice ± SD for each group. (B) Tumor xenografts of CFPAC-1 cells were surgically excised 5, 24, or 48 hr after buffer or TOP3 injection, and stained with anti-pimonidazole antibody. To calculate the percentage of hypoxic regions, the percentage of pimonidazole-positive cells to a whole solid tumor was quantified with NIH Image 1.63 software. Results are the mean of three to four tumors from independent tumor-bearing mice ± SD for each group. *p < .01. (C) Buffer-treated (a–f) and TOP3-treated (g–o) CFPAC-1 xenografts were surgically excised at the indicated times after the treatments, and serial sections were stained with anti-pimonidazole antibody (a, d, g, j, and m), HE (c, f, i, l, and o), or secondary antibody only as a negative control (NC; b, e, h, k, and n). Three to four tumors from independent tumor-bearing mice were examined for each treatment group and representative tumor sections are shown. Bar = 1 mm. The areas squared in f and o are applied to Figure 6A–C and Figure 6D–6F, respectively.*

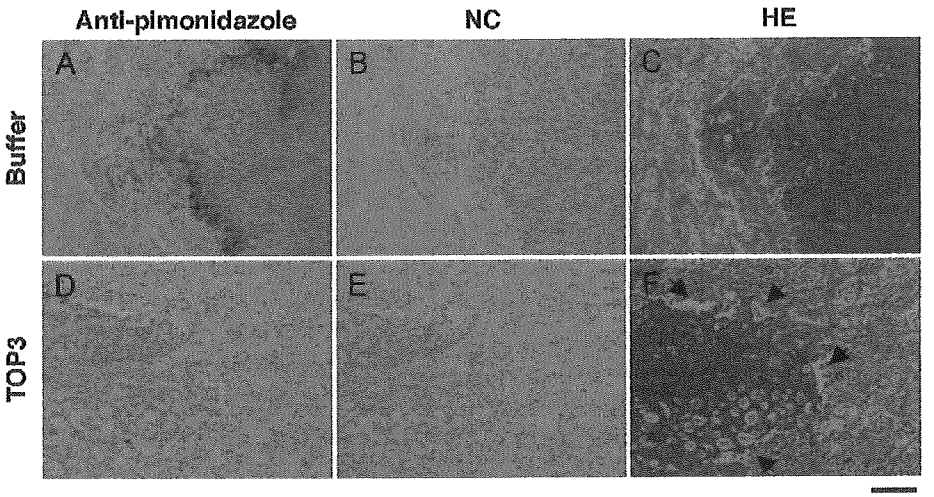

Figure 6. *Effect of TOP3 on hypoxic/HIF-1-expressing cells in xenograft. The areas squared in Figure 5Cf and Co are magnified and shown in A–C and D–F, respectively. Buffer-treated (A–C) and TOP3-treated (D–H) CFPAC-1 xenografts were stained with HE (C and F), anti-pimonidazole antibody (A and D) and without primary antibody as a negative control (NC; B and E). Bar = 100 μm. Arrow = empty spaces between viable region and necrotic region.*

The immunohistochemical analysis using anti-luciferase antibody and anti-pimonidazole antibody indicated that the locations of the luciferase-expressing cells and the pimonidazole-positive cells were very similar. Both of them were located at the boundary areas between viable cells and necrotic regions (Figure 2A). However, their content and intensity were slightly different. The areas where luciferase was expressed were significantly wider than the ones where pimonidazole-positive cells were located. Because the oxygen concentration decreases as the distance from the blood vessels increases, HIF-1α stabilization may have occurred under milder hypoxic conditions than the binding of pimonidazole compounds with thiol groups in proteins, which occurs in less than 10 mmHg [38] (www.radonc.unc.edu/pimo/main.htm). Although oxygen-dependent regulation is the major regulation for HIF-1α expression, we must consider that HIF-1 expression is also affected by oxygen-independent regulation [39,40], and pimonidazole reactivity is absolutely oxygen-dependent [31,38]. Because HIF-1 activity is closely associated with malignant progression [5,16], monitoring HIF-1 activity in solid tumors is crucial for cancer therapy.

Because TOP3 stability is regulated by the same oxygen-dependent mechanism as HIF-1α protein through common ODD domain, both TOP3 and HIF-

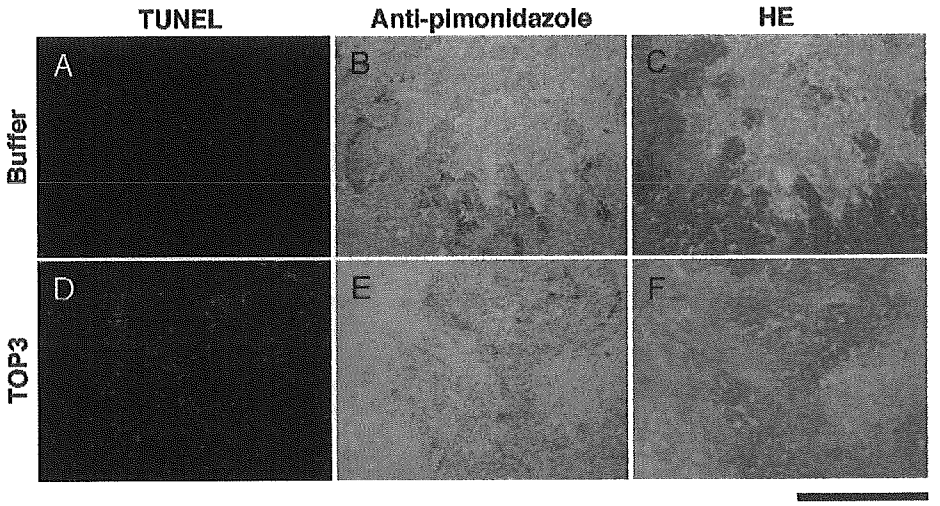

Figure 7. *Apoptosis of hypoxic/HIF-1-expressing cells in TOP3-treated tumor xenograft. CFPAC-1 xenografts excised at 12 hr after either buffer (A–C) or TOP3 (D–F) administration were stained for TUNEL (A and D). Serial tumor sections were stained with anti-pimonidazole antibody (B and E) and HE (C and F). Three tumors were examined for each treatment group and representative tumor sections are shown. Bar = 1 mm.*

1α must be stabilized in the same hypoxic tumor cells in vivo as well as in vitro. Therefore, TOP3 is expected to target HIF-1α-expressing hypoxic tumor cells, leading to shutting off the HIF-1-induced gene expression. In accordance with this expectation, the disappearance of pimonidazole-positive cells from TOP3-treated tumor sections (Figures 5B,C, 6D, and 7E) and the existence of empty spaces between viable and necrotic regions in the TOP3-treated tumor sections (Figure 6D–F) strongly suggests the elimination of hypoxic/HIF-1-expressing cells after TOP3 treatment. Although the disappearance of these areas may be a consequence of the removal of fragile apoptotic cells from the section during the staining process, TOP3-targeted cells must be removed in vivo because the total tumor mass and the photon counts of HeLa/5HRE-Luc xenografts were significantly reduced after TOP3 administration (Figure 4B and C). Although the precise mechanism underlying the removal of hypoxic tumor cells by TOP3 in vivo has not been investigated, it is likely that such cells initially undergo apoptosis, as shown in vitro [23] and in vivo (Figure 7), and that they might be removed by macrophages attracted by the caspase-3-induced "eat-me signal" [41].

TOP3 did not influence luciferase–luciferin reaction in vitro (data not shown). The bioluminescent signals from HeLa/EF-Luc were not so significantly decreased as the one from the HeLa/5HRE-Luc xenografts of TOP3-treated mice (Figure 4C). These results indicate that the significant decrease of the bioluminescent signals from HeLa/5HRE-Luc xenografts of TOP3-treated mice was not simply due to interference of TOP3 in luciferase–luciferin reaction in vivo. Low oxygen concentration influences the luciferin reaction, and thus, we cannot simply compare the bioluminescent signals from HeLa/EF-Luc xenografts with the one from HeLa/5HRE-Luc xenografts. However, as long as monitoring the same HeLa/5HRE-Luc xenografts, the change in the bioluminescent intensity should reflect the amount of hypoxic tumor cells.

The first TOP3 administration caused the most significant reduction in HIF-1 activity on Day 3 (Figure 4B and C). Because HeLa/5HRE-Luc cells had little luciferase activity under aerobic conditions in vitro (Figure 1A), the photon counts detected in the TOP3-treated xenografts on Day 3 may have been background (Figure 4B and Ce). If so, almost all HIF-1-expressing cells were removed as the results of the first administration. The sequential administration with TOP3 in 5-day intervals resulted in remarkable suppression of the increase in the bioluminescence from HeLa/5HRE-Luc xenografts. The relative photon counts from buffer-treated HeLa/5HRE-Luc tumors reached 22-fold, whereas the ones from TOP3-treated tumors were still suppressed on Day 15 (Figure 4B and C). All of these results strongly suggest that the optical imaging of HIF-1 activity by a luciferase reporter system can contribute to the screening and the development of HIF-1-targeting drugs and the convenient evaluation of the efficacy of anti-cancer therapy on tumor hypoxia.

In optical imaging, there was a time lag between the decrease in the photon counts and the elimination of the pimonidazole-positive cells after TOP3 treatment (Figures 4A–C, 5B and C). Concretely, after the first TOP3 administration on Day 0, the tumor became the smallest on Day 2 (Figure 4A) and the pimonidazole-positive cells decreased within 2 days (48 hr; Figure 5B and C), whereas relative photon counts became the lowest on Day 3 (Figure 4B and C). Although luciferase expression is initiated by a hypoxic stimulus, luciferase activity remains even after the surrounding conditions change to aerobic until the protein is degraded. Hence, monitoring the HIF-1 activity as a luciferase activity may not be always punctual. Therefore, it is necessary to further improve the reporter system to realize real-time imaging.

Acknowledgments

We thank Dr. S. Kimura (Kyoto University, Kyoto, Japan) and S. Watanabe (SC BioScience) for IVIS technical support; N. Murakami-Harada, E. Nishimoto, and A. Morinibu for skilled technical assistance. This work was supported by research grants from the Ministry of Education, Science, Sports, and Culture of Japan and Kyoto City Collaboration of Regional Entities for the Advancement of Technological Excellence, JST.

References

[1] Vaupel P, Kallinowski F, Okunieff P (1989). Blood flow, oxygen and nutrient supply, and metabolic microenvironment of human tumors: A review. *Cancer Res.* **49**:6449–6465.

[2] Brown JM (2000). Exploiting the hypoxic cancer cell: Mechanisms and therapeutic strategies. *Mol Med Today.* **6**:157–162.

[3] Teicher BA (1994). Hypoxia and drug resistance. *Cancer Metastasis Rev.* **13**:139–168.

[4] Hockel M, Vaupel P (2001). Tumor hypoxia: Definitions and current clinical, biologic, and molecular aspects. *J Natl Cancer Inst.* **93**:266–276.

[5] Harris AL (2002). Hypoxia—a key regulatory factor in tumour growth. *Nat Rev Cancer.* **2**:38–47.

[6] Hockel M, Schlenger K, Aral B, Mitze M, Schaffer U, Vaupel P (1996). Association between tumor hypoxia and malignant progression in advanced cancer of the uterine cervix. *Cancer Res.* **56**:4509–4515.

[7] Giaccia AJ (1996). Hypoxic stress proteins: Survival of the fittest. *Semin Radiat Oncol.* **6**:46–58.